

Optics systems for the home laboratory: caveat emptor

**Cheng Yang, Adam Courville and
Joseph D. Ferrara***

Molecular Structure Corporation, The Woodlands, Texas, USA

Correspondence e-mail: jdf@msc.com

A careful and detailed evaluation of different multilayer optics (Osmic Cross-coupled Max-Flux Optics and Osmic Confocal Max-Flux Optics) compared with MSC/Yale Total-Reflection Mirrors has been completed. This report provides a detailed comparison of usable flux, spectral purity, divergence, beam profile and data quality for these systems. The most striking results have been obtained using either the Osmic #4 or #7 Confocal Max-Flux Optic, which were designed for 0.1 and 0.2 mm focal spots, respectively, in conjunction with a 0.3 mm focal spot. These optic configurations provide a 5.8-fold and 8.2-fold increase in flux through a 0.2 mm aperture, respectively, compared with the MSC/Yale Mirrors.

Received 18 March 1999

Accepted 28 July 1999

1. Introduction

Recently, the protein crystallographic community has shown considerable interest in graded multilayer optics as produced by Osmic Inc. (Grupido & Remus, 1998). Bruker introduced the first commercial product to utilize this technology, Göbel Mirrors (Schuster & Göbel, 1995), several years ago. This product incorporates two Osmic multilayers arranged sequentially and perpendicular to each other in much the same configuration as a Total-Reflection (TR) mirror system (Kirkpatrick & Baez, 1948; Franks, 1955). The advantages of this system over a TR system are that the beam is nearly parallel and is nearly monochromatic. The disadvantage is that the beam is 2.5 times larger (approximately 0.8×0.8 mm) than that of a TR system and thus the useable flux for protein crystallography is less.

At the 1997 ACA meeting, Osmic announced a new multilayer product called the Confocal Max-Flux Optic (Fig. 1). In this optic product, two graded multilayer optics are glued together in a perpendicular orientation. The advantage of this system is that both optics are the same distance from the X-ray source and thus capture a larger view of the source, resulting in a higher-flux beam. The standard Confocal Max-Flux utilizes elliptical optics, resulting in a fixed focused beam. A focused beam has the advantage of providing more useable flux on the crystal at the expense of introducing divergence into the beam.

Confusion has arisen because Osmic manufactures a number of different models of the Confocal Max-Flux Optic. The curvature and associated variation in grading are calculated to fit the size of the X-ray source and the distance of the optic from the source and to make every point satisfy Bragg's Law. Osmic produces three different models of this type of optic, designed to work best with 0.1, 0.2 or 0.3 mm cathodes. These optics were designed using theoretical ray-tracing calculations and, prior to the following experiments, had not

been carefully characterized in a controlled environment. Instead, the various configurations have been installed in different laboratories and each has performed a different set of validation tests.

As a supplier of Max-Flux Optics, we have spent a considerable amount of time characterizing the performance of the various configurations of the new optic with alignment hardware and collimators manufactured by MSC. By using the same generator and detector, and utilizing the same set of test criteria, we have sought to make the results self-consistent and easily interpretable. In general, we have found that the empirical results do not match the theoretical values as described by Osmic.

In this report, we describe the testing of the multilayer optics with comparisons drawn to TR optics.

2. Background

X-ray optics are used to condition the X-ray beam in order to improve data quality. This conditioning can be as simple as using an aperture to limit the X-ray beam or as complex as using a graded multilayer monochromator. An ideal X-ray beam for the home laboratory would have high flux, would have a cross-section equal to or slightly larger than the sample, would be nearly parallel and would be monochromatic. Since current technology makes it difficult to provide all four properties for the home laboratory, optics systems are a careful balance of the above properties. High flux and a small-diameter beam mean smaller crystals may be analyzed. A nearly parallel beam means the spot shape is nearly invariant at all crystal-to-detector distances. A monochromatic beam reduces X-ray background. All these properties improve data quality by enhancing the signal-to-noise ratio. The methods by which these optics condition the X-ray beam is described in the literature and will not be described here (Roberts & Parrish, 1968; Witz, 1969; Arndt & Sweet, 1977; Arndt, 1990).

We have characterized several commercially available optics systems in an objective manner so that one can choose the appropriate optics system based on empirical results and not just theoretical calculations. The MSC/Yale Mirror configuration was chosen as a reference because it is the most common optics system found in macromolecular crystallography laboratories today. The MSC Cross-coupled, MSC Green-3, MSC Purple-2 and MSC Blue-1 Optics Configurations

are based on standard optics configurations recommended by Osmic. We also studied combinations of optics and sources not recommended by Osmic. The MSC Blue-3 Optics Configuration is the result of a serendipitous discovery that the Osmic #4 Confocal Max-Flux Optic, which is theoretically optimized for a 0.1 mm focal spot, actually performs substantially better when coupled with a 0.3 mm focal spot. Likewise, the MSC Purple-3 Optics Configuration incorporating the Osmic #7 Confocal Max-Flux Optic designed for a 0.2 mm source performs better than the recommended configuration, when used in conjunction with a 0.3 mm focal spot. Table 1 provides a description of the geometry of the optics configurations studied.

3. Experimental

To quantify the four properties described above, we have studied the spatial, spectral and intensity properties of the X-ray beams produced by MSC/Yale Mirrors focused at the crystal position, MSC/Yale Mirrors focused at 350 mm, the MSC Cross-coupled Optics Configuration and the MSC Green, Blue and Purple Optics Configurations. Data sets were collected on three different protein crystals in order to examine how the different optics configurations behave in the crystallographic experiment.

3.1. General

For this study, the MSC/Yale Total-Reflection Mirrors described in Table 1 were used, as designed by Z. Otwinowski and J. Johnson of Yale University, and manufactured by MSC. The MSC/Yale mirror system has one horizontal platinum-coated mirror and one vertical nickel-coated mirror in a Kirkpatrick–Baez configuration. Opposite the center point of each mirror was a single knife-edge used for eliminating the direct beam. The entire mirror system was installed at a 6° take-off angle and was purged with helium gas. The most significant advantage of the MSC/Yale mirror system is the ability to change the focus. The MSC/Yale Mirrors were focused at the desired position by maximizing the intensity through a 0.5 mm aperture at the sample position or at 350 mm.

The MSC Cross-coupled Optics Configuration was integrated with MSC alignment hardware in the Osmic recommended configuration as described in Table 1. An Osmic GO-11 was mounted in a vertical orientation and an Osmic GO-13 was mounted in a horizontal orientation. The housings had 5 mm input and output windows for the X-ray beam. The configuration was aligned to the anode with a 6° take-off angle and purged with helium gas.

The MSC Green, Blue and Purple Optics Configurations

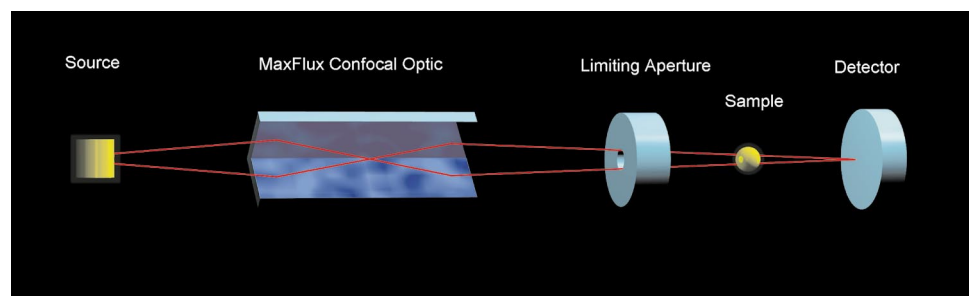


Figure 1
A schematic representation of an Osmic Confocal Max-Flux Optic.

Table 1

A description of the optics configurations tested.

	Cathode size (mm)	Power (kW)	Optic	Distance from center of optic to source (mm)	Collimator	Distance from source to aperture (mm)
MSC/Yale mirrors focused at the crystal position and focused at 350 mm	0.3	5.0	80 mm Pt-coated	130	1.0 mm rear aperture	393
			160 mm Ni-coated	253	0.5 mm front aperture	500
MSC Cross-coupled Optics Configuration	0.3	5.0	Osmic GO-11	90	1.0 mm rear aperture	580
	0.3		Osmic GO-13	150	1.0 mm front aperture	685
MSC Green-3 Optics Configuration	0.3	5.0	Osmic #1 Confocal	240	2.0 mm rear aperture	450
					0.5 mm front aperture	590
MSC Purple-1 Optics Configuration	0.1	1.0	Osmic #7 Confocal	200	No rear aperture	260
MSC Purple-2 Optics Configuration	0.2	3.0			0.5 mm front aperture	400
MSC Purple-3 Optics Configuration	0.3	5.0				
MSC Blue-1 Optics Configuration	0.1	1.0	Osmic #4 Confocal	120	2.0 mm rear aperture	230
MSC Blue-2 Optics Configuration	0.2	3.0			0.5 mm front aperture	370
MSC Blue-3 Optics Configuration	0.3	5.0				

used either a #1, #4, or #7 Confocal Max-Flux Optic with side-by-side geometry (Fig. 1). The optic is mounted in MSC-designed alignment hardware with a 45° rotation around the X-ray beam to make the beam nearly horizontal. There are two 1.2 mm square windows on each side of the optic housing for X-ray input and output. The distances from the source to the center of the optic and to the apertures defining the collimator are given in Table 1 and are based on theoretical calculations by Osmic. The configurations were set at a 6° take-off angle and flushed with helium gas. For the MSC Green and Blue Optics Configurations, a collimator with a 1.0 mm rear aperture and a 0.5 mm front aperture was used. The collimator used in the MSC Purple Optic Configurations has a single 0.5 mm front aperture. Tests on the MSC Purple Optic Configuration with a 1.0 mm rear aperture and a 0.5 mm front aperture are in progress and will be presented at a later date.

All tests were performed on a Rigaku RU-H2R rotating-anode generator. The generator was run at 50 kV and 100 mA for the 0.3 mm cathode, 50 kV and 60 mA for the 0.2 mm cathode and 50 kV and 20 mA for the 0.1 mm cathode. Optimal bias settings for each cathode were determined using 10 µm pinhole images. A Rigaku R-AXIS IV image-plate detector was used for data collection. In all experiments, the only variable is the type of optics configuration used.

It should be noted the MSC Cross-coupled Optics Configuration was the first optics system tested and the procedures used to measure the properties of the optics had not been fully developed. Not all tests were made on this optics configuration, and the measurements which were made were not performed in the same fashion as the other optics tested. Where results are presented for the MSC Cross-coupled Optics Configuration, they are corrected for any differences caused by experimental procedures. The exception to this was the data collection on myoglobin, which was performed under the same conditions as for the other optics systems (MSC/Yale Mirrors and MSC Green-3 Optics Configuration).

In order to compare the consistency of performance of optics provided by Osmic, three of the #1 optics were set up on an RU-H3R (MSC Green Optics Configuration A, B and C). For optics A, B and C, the useable flux was measured and scaled to the intensity measurement of optic A as tested on the RU-H2R. Optic A was the first Osmic #1 optic delivered to MSC and all tests were performed on this optic.

3.2. Spectral purity

Spectral purity was determined by placing an AMPTEK XR-100T in the center of the direct beam and attenuating the direct beam with a 0.01 mm aperture and a slit to give approximately 200 counts s⁻¹. It is important to keep the count rate low so that coincident photons do not pile up and add noise to the spectra between λ and $\lambda/2$. The percentages of each radiation present were calculated by integrating the photon counts in the region of interest and dividing by the total number of photons observed. Spectra recorded for the MSC Cross-coupled Optic Configuration are very noisy and not as reliable as the other spectra because the count rates were too high and pile-up of photons occurred.

3.3. Useable flux

We define useable flux as the flux per unit area weighted by the percentage of Cu $K\alpha$. To measure useable flux, tantalum apertures of 0.5, 0.3 and 0.2 mm were placed at the crystal position. The translation and rotation of each aperture was adjusted to give maximum intensity on an MSC-manufactured PIN-diode detector. In the case of the MSC Green-3 Optics Configuration, three optics (A, B and C) were tested with the same alignment hardware and collimator on an RU-H3R and results scaled to measurements of optic A on the standard RU-H2R.

3.4. Divergence

For the MSC Cross-coupled Optics Configuration, direct-beam images were taken at crystal-to-detector distances of

100, 200, 300 and 400 mm. For the remaining configurations, direct-beam images were taken at crystal-to-detector distances of 100, 110, 120, 130, 200, 300, 400 mm. For all measurements, an R-AXIS IV detector with Fuji BAS-III image plates was used. The full-width at half-maximum (FWHM) was determined by finding the maximum for each peak, calculating the lines through the points above and below half the peak value on both sides of the maximum and calculating the points of intersection of these lines with the line at half-maximum. This method allows for non-uniformity in the beam profile while still giving accurate results automatically. The FWHM values used are the average of at least three and typically five observations.

3.5. Beam profile at the crystal position

For all optics configurations except the MSC Cross-coupled Optics Configuration, the beam profile was determined by placing a 0.005 mm platinum aperture in an *xy* stage. The pinhole was scanned across the beam at the crystal position in 0.05 mm increments. The flux passing through the pinhole was measured with a scintillation counter and PHA optimized for Cu $K\alpha$ radiation. For each point in the profile, ten 1 s counts were taken and averaged.

For the MSC Cross-coupled Optics Configuration, a 0.01 mm brass aperture was scanned across the beam in 0.1 mm increments. The intensity data were collected with an AMPTEK XR-100T and corrected for non-linearity. The profile was scaled to be consistent with the intensity, *via* the pin-diode detector, of the Blue-3 Optics Configuration.

3.6. Data collection

3.6.1. Myoglobin. Data sets were collected on a single crystal of P6 myoglobin with the MSC/Yale Mirrors focused at the crystal position, the MSC Cross-coupled Optics Configuration and the MSC Green-3 Optics Configuration. The crystal-to-detector distance was 120 mm. Two scans (inverse beam) of 60 1.5°, 75 s oscillation images were taken. All data were processed with *HKL* (Otwinowski & Minor, 1997) and gave an overall completeness of 96.4% in the resolution range

20–1.8 Å, with 93.7% completeness in the 1.86–1.80 Å shell. Anomalous difference Patterson maps were calculated with *XtalView* (McRee, 1992).

3.6.2. Thaumatin. Data sets were collected on a frozen thaumatin crystal at 93 K on the R-AXIS IV, with the MSC/Yale Mirrors focused at the crystal position, the MSC/Yale Mirrors focused at 350 mm and the MSC Green-3 Optics Configuration. The crystal-to-detector distance was 120 mm. Oscillation images of 0.5° were taken for 6 min. All data were processed with *HKL* and gave an overall completeness of 96.5% in the resolution range 50–1.8 Å, with 96.7% completeness in the 1.86–1.80 Å shell. An attempt was made to collect a fourth data set for the MSC Blue-3 Optics Configuration; however, the mosaicity of the sample increased from 0.45 to 0.65°, indicating that the crystal was no longer suitable.

3.6.3. Proprietary protein. Five data sets were collected on a frozen proprietary protein crystal with cell lengths less than 100 Å. The crystal-to-detector distance was 150 mm for the MSC Green-3 Optics Configuration and 120 mm for the MSC Purple-3 and Blue-3 Optics Configurations. Oscillation images of 8 min per 0.5° were collected. The data were processed with *HKL* and gave at least 97.8% completeness in the highest resolution shell.

4. Results and discussion

The spectral properties of the X-ray beam impinging on the crystal are important. White radiation causes higher backgrounds, reducing the signal-to-noise ratio. White-radiation streaks can cause erroneous background calculations for individual reflections. Finally, white radiation may enhance crystal decay. Cu $K\beta$ radiation can cause reflections to appear at a *d*-spacing 90% of the *d*-spacing of a reflection, making systematic absences appear present.

Figs. 2 and 3 display representative energy spectra observed for the MSC/Yale Mirrors and the MSC Green-3 Optics Configuration. Qualitatively, one can readily see that the multilayer optic produces little white radiation and effectively no Cu $K\beta$ (8.9 keV) radiation compared with the MSC/Yale Mirrors. All multilayer optics produce a trace of Fe $K\alpha$ at

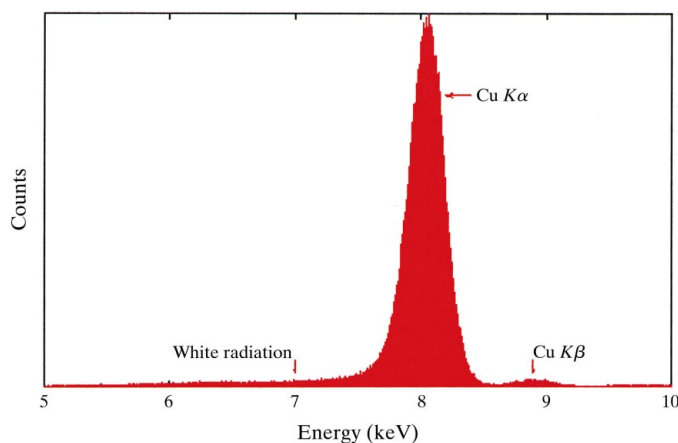


Figure 2
Energy spectrum for the MSC/Yale Mirrors focused at 350 mm.

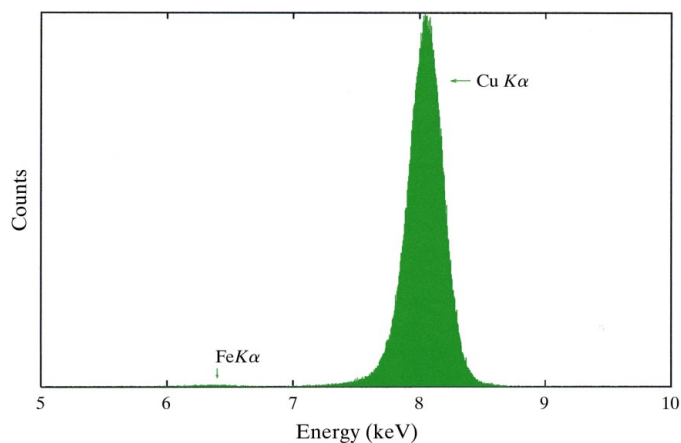


Figure 3
Energy spectrum for the MSC Green-3 Optics Configuration.

Table 2

Comparison of the spectral properties of the MSC/Yale Mirrors and MSC Green, Purple and Blue Optics Configurations.

	Cu $K\alpha$ (%)	Cu $K\beta$ (%)	Fe $K\alpha$ (%)	White radiation (%)
MSC/Yale Mirrors focused at the crystal position	86.5	1.5		12.0
MSC/Yale Mirrors focused at 350 mm	89.2	1.4		9.4
MSC Green-3 Optics Configuration	97.4	0.013	0.28	2.30
MSC Blue Optics Configuration	97.8 (5)	Not measurable	0.22 (3)	2.1 (6)
MSC Purple Optics Configuration	96.3 (1)	Not measurable	0.22 (2)	3.5 (2)

6.4 keV. It is postulated that this arises from fluorescence of the stainless steel carrier used to support the optic. For the calculation of the percentage of Cu $K\alpha$, a width of 8.050 ± 0.382 keV of was used. This was taken from the half width at 1% on the high-energy side of the MSC/Yale Mirrors focused at the crystal position. Percentages of white radiation, Cu $K\alpha$, Cu $K\beta$ and Fe $K\alpha$ are given in Table 2. The spectrum of the MSC Cross-coupled Optics Configuration indicates the presence of Cu $K\beta$ at a level of about 0.1%.

The divergence of the X-ray beam is important; a parallel beam is ideal. An X-ray beam with divergence increases the effective thickness of the Ewald sphere, making more reflections visible at any given time. This increases spot size and the chance that spots may overlap. In order to measure diffraction data accurately, the reflections should be resolved; that is, background should be present between reflections. In order to resolve reflections for samples with large unit cells, a longer crystal-to-detector distance is needed. However, if the divergence is too great then the spots become larger more quickly than the separation between spots as the crystal-to-detector distance increases. Increased spot size also increases the background under reflections, therefore decreasing signal-to-noise. This makes for a tricky balancing act where one must select the crystal-to-detector distance which gives the best spot resolution.

Figs. 4 and 5 show the full-width at half-maximum of the direct beam *versus* crystal-to-detector distance in the horizontal and vertical directions, respectively, for all the optics

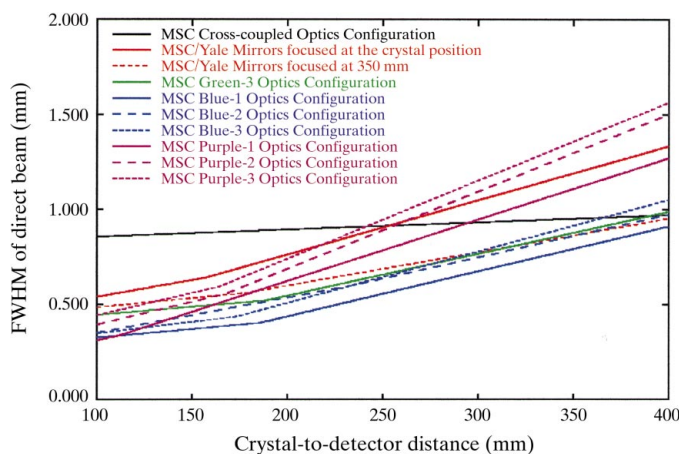


Figure 4

Plots of the full-width at half-maximum in the horizontal direction for each of the optics configurations.

systems. The slope of each line yields the divergence of the optic. It is interesting to note that the MSC/Yale Mirrors (in the horizontal direction only) and the MSC Green, Purple and Blue Optic Configurations, all focusing optics systems, present a divergence which is low near the crystal and increases after a certain point. This inflection

point is typically in the crystal-to-detector distance range 50–200 mm. The X-ray beams in these optics systems are not observed to be convergent prior to the focal point and divergent afterwards, as one might expect for a focusing optics system.

Detailed performance calculations for the MSC Blue-3 Optics Configuration, which include non-ideality of the source, a reasonable figure error for the optic and the

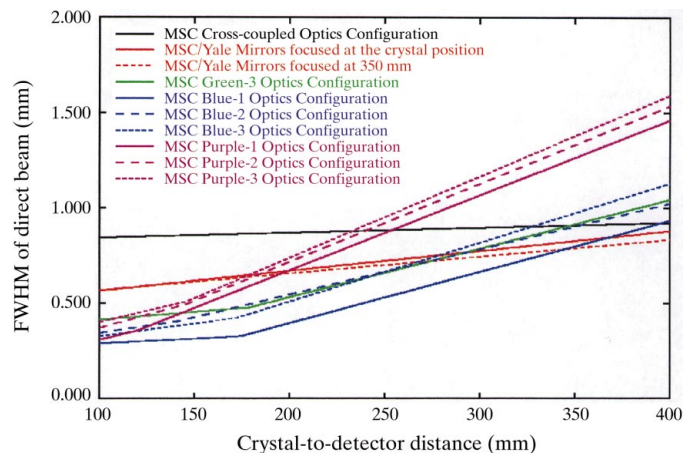


Figure 5

Plots of the full-width at half-maximum in the vertical direction for each of the optics configurations.

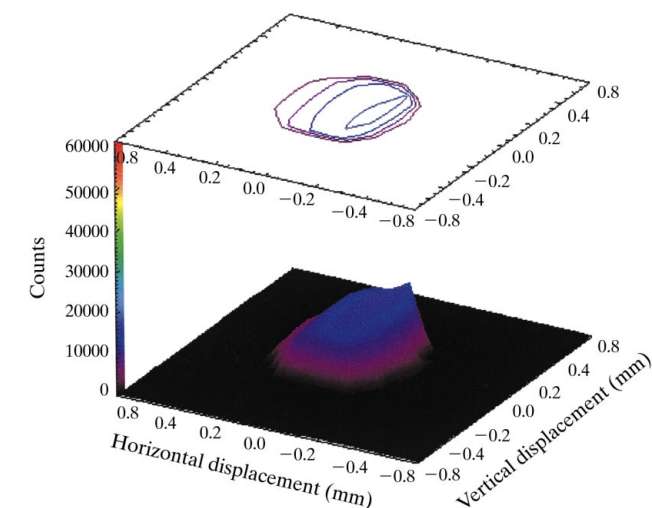


Figure 6

Beam profile of the MSC/Yale Mirrors focused at the crystal position. Contour levels are drawn at 4000 counts.

Table 3

Comparison of the useable flux of the MSC/Yale Mirrors and MSC Green, Blue and Purple Optics Configurations.

	0.5 mm aperture	0.3 mm aperture	0.2 mm aperture
MSC/Yale Mirrors focused at 350 mm	1.00	1.00	1.00
MSC/Yale Mirrors focused at the crystal position	1.24	1.09	1.92
MSC Green-3 Optics Configuration	A 1.98, B 2.93, C 2.57	A 2.12, B 3.20, C 2.73	A 3.69, B 5.41, C 4.47
MSC Blue-1 Optics Configuration	1.73	2.00	4.00
MSC Blue-2 Optics Configuration	2.36	2.62	4.50
MSC Blue-3 Optics Configuration	3.66	3.63	5.85
MSC Purple-1 Optics Configuration	1.23	2.01	4.59
MSC Purple-2 Optics Configuration	2.62	3.86	7.62
MSC Purple-3 Optics Configuration	3.22	3.92	8.23

geometry described in Table 1 (Jiang, 1999), are consistent with the experimentally observed data. It is predicted the divergence below a crystal-to-detector distance of 180 mm is 1.5 mrad and above 180 mm is 3.4 mrad. The experimental results are 1.1 (2) mrad and 2.7 (2) mrad, respectively. It is the limiting aperture near the optic which is the cause of the small

positive divergence, rather than convergence, near the focal point.

Macromolecular samples are often quite small. The size of the sample determines the amount of flux illuminating the sample. In order to quantify this useable flux impinging on the sample for different crystal sizes, several apertures were placed at the crystal position. To clarify the improvements of useable flux for the various optics, the ratios of the flux for the MSC/Yale Mirrors focused at 350 mm to each of the other optic systems were calculated for apertures of 0.5, 0.3 and 0.2 mm and weighted by the percentage of Cu $K\alpha$. These results are presented in Table 3. The data for the MSC Green Optics Configuration on the RU-H3R (optics B and C) were scaled to be consistent with the results on optic A on the RU-H2R. A dramatic increase in useable flux is visible for the 0.3 and 0.2 mm apertures over the MSC/Yale Mirrors focused at 350 mm.

Another interesting feature is the spot size itself. The MSC Purple-1 Optic Configuration provides the smallest beam size for crystal-to-detector distances of less than 110 mm. This suggests that for most data-collection strategies the MSC Purple Optic Configuration will provide better spot resolution than the other optics systems for crystal-to-detector distances less than 110 mm. The MSC Blue Optic Configurations provide the smallest beam size, from 110 mm to about 250 mm. This range of distances is typical of most data

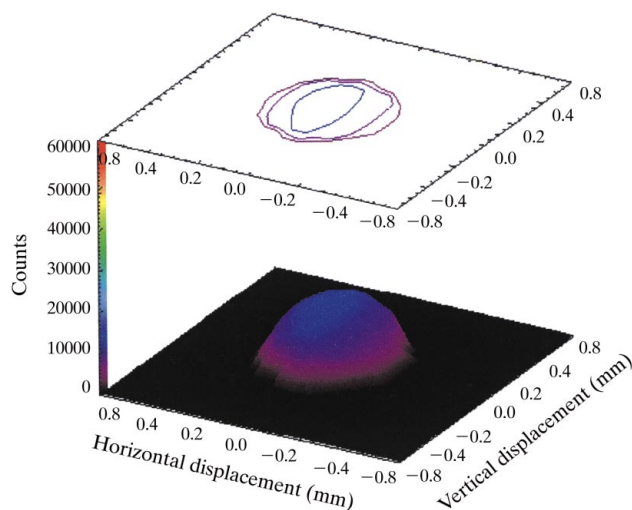


Figure 7
Beam profile of the MSC/Yale Mirrors focused at 350 mm.

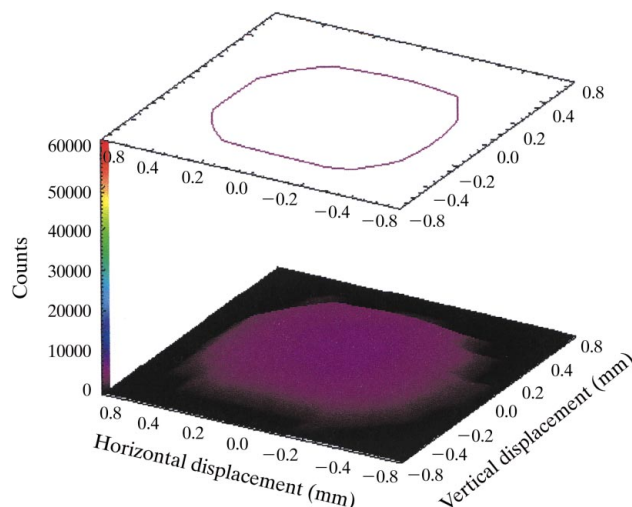


Figure 8
Beam profile of the MSC Cross-Coupled Optics Configuration.

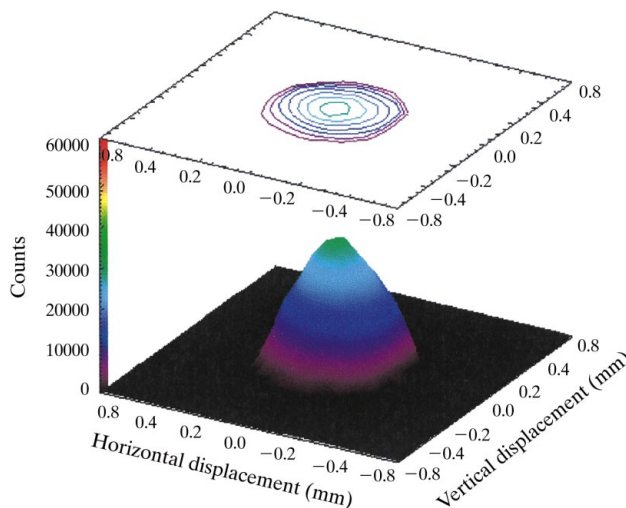


Figure 9
Beam profile of the MSC Green-3 Optics Configuration.

Table 4

Comparison of statistics for data sets on a myoglobin crystal collected with MSC/Yale Mirrors focused at the crystal position, the MSC Cross-coupled Optics Configuration and MSC Green-3 Optic Configuration.

	I/σ	I/σ (1.86–1.80 Å)	$\langle I \rangle$	R_{merge}
MSC/Mirrors focused at the crystal position	35.5	9.6	1574.7	4.7
MSC Cross-coupled Optics Configuration	33.0	7.1	820.7	5.1
MSC Green-3 Optics Configuration	35.7	12.0	3230.2	4.4

Table 5

Comparison of the anomalous difference Patterson maps for data sets on a myoglobin crystal collected with MSC/Yale Mirrors focused at the crystal position, the MSC Cross-coupled Optics Configuration and MSC Green-3 Optics Configuration.

The anomalous difference Patterson maps were calculated using *XtalView* and data from 5.0 to 2.0 Å.

	Peak 1	Peak 2	Peak 3
MSC/Yale Mirrors focused at the crystal position	33.0	39.0	15.6
MSC Cross-coupled Optics Configuration	30.0	34.7	15.5
MSC Green-3 Optics Configuration	38.4	44.1	19.9
Theoretical peak heights	52.8	60.8	26.8

Table 6

Comparison of data sets on a single thaumatin crystal with MSC/Yale Mirrors and the MSC Green Optics Configuration.

	I/σ	I/σ (1.86–1.80 Å)	$\langle I \rangle$	R_{merge}
MSC/Yale Mirrors focused at the crystal position	17.0	3.6	831.2	6.8
MSC/Yale Mirrors focused at 350 mm	17.0	3.6	815.7	6.1
MSC Green-3 Optics Configuration	20.5	5.3	1619.2	4.7

collection in our application laboratory. The divergence of the MSC Cross-coupled Optic Configuration is the lowest of all the systems; however, this occurs at the expense of useable flux, which will be shown later.

The profiles of the beams at the crystal position are shown in Figs. 6–14. The figures have been drawn so the reader can

easily compare the spatial distribution of intensity. The MSC/Yale Mirrors, Figs. 6 and 7, display a broad, flat profile with fine structure added by the mirrors themselves. The MSC Cross-coupled Optics Configuration, Fig. 8, clearly shows a very large diffuse maximum, good for crystals of 0.8 mm or larger. It should be obvious, even though the aperture experiments were not performed for this configuration, that the useable flux for small crystals for this system is quite low. The MSC Green-3 Optics Configuration, Fig. 9, displays a conical profile, which explains the higher useable flux, as compared to the MSC/Yale Mirrors and MSC Cross-coupled shown in Table 3. The MSC Purple-2 and Purple-3 Optics Configurations, Figs. 10 and 11, display a sharper conical profile and higher useable flux than the previous configurations. The MSC Blue-1 and Blue-2 Optics Configurations, Figs. 12 and 13, present a somewhat lopsided profile with some fine structure.

It is clear from the profiles that the MSC Blue-3 Optics Configuration (Fig. 14) produces a very desirable profile. It is quite uniform and has a large maximum of diameter 0.3 mm. The

useable flux is consistent with the measurements in Table 3. The profile of the MSC Purple-3 Optics Configuration provides more useable flux for small crystals. However, this is at the expense of divergence. The integrated intensity of the two profiles is the same within a few percent. The profile of a spot on the detector is the convolution of the profile of the

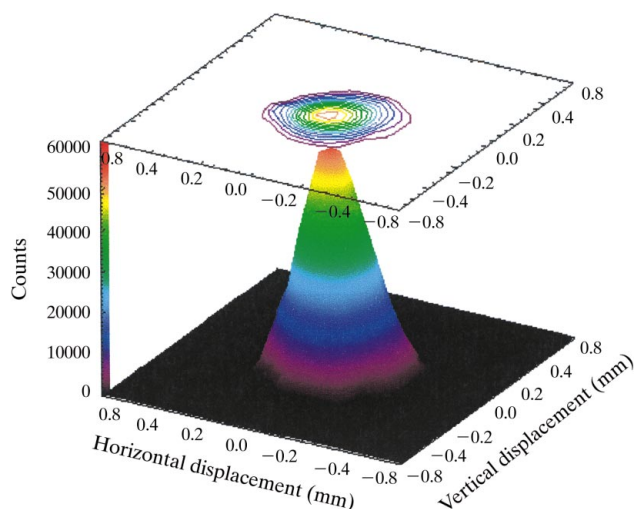


Figure 10
Beam profile of the MSC Purple-2 Optics Configuration.

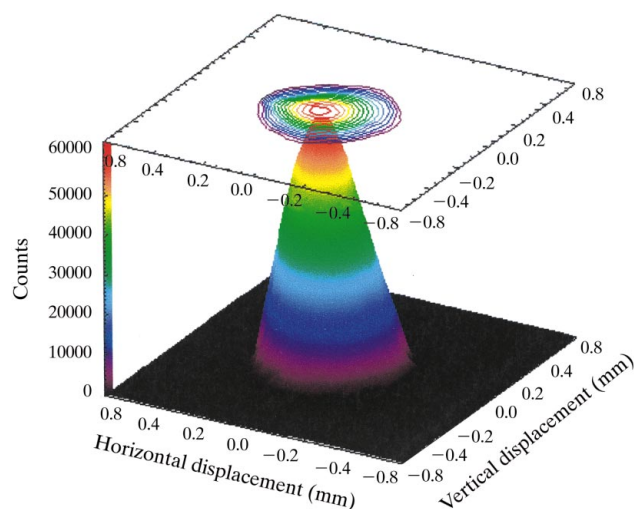


Figure 11
Beam profile of the MSC Purple-3 Optics Configuration.

Table 7

Comparison of data sets on a single proprietary crystal collected with the MSC Green-3, Purple and Blue Optics Configurations.

MSC Blue-3 Optics Configuration data set No. 2 was collected to verify the crystal quality was consistent with the first MSC Blue-3 Optics Configuration data set.

	I/σ	I/σ (1.97–1.90 Å)	$\langle I \rangle$	R_{merge}
MSC Green-3 Optics Configuration	19.1	9.8	16364.3	4.9
MSC Blue-1 Optics Configuration	18.4	11.0	16286.8	3.1
MSC Blue-3 Optics Configuration	20.7	11.9	22000.4	2.9
MSC Purple-3 Optics Configuration	19.5	12.4	46359.2	4.2
MSC Blue-3 Optics Configuration (No. 2)	20.0	11.5	21789.2	3.7

direct beam and the crystal. The profiles of these optics systems are symmetrical and free of fine structure. The result will be better spot shapes observed at the detector.

The results of data collection on myoglobin, thaumatin and a proprietary protein crystal are given in Tables 4, 5, 6 and 7. It

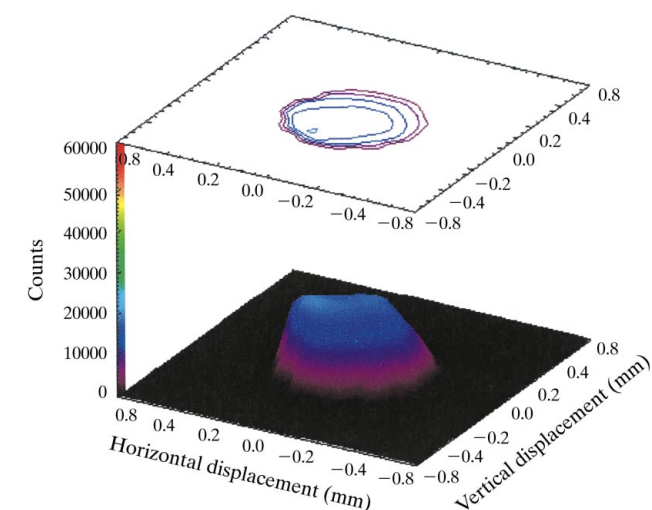


Figure 12
Beam profile of the MSC Blue-1 Optics Configuration.

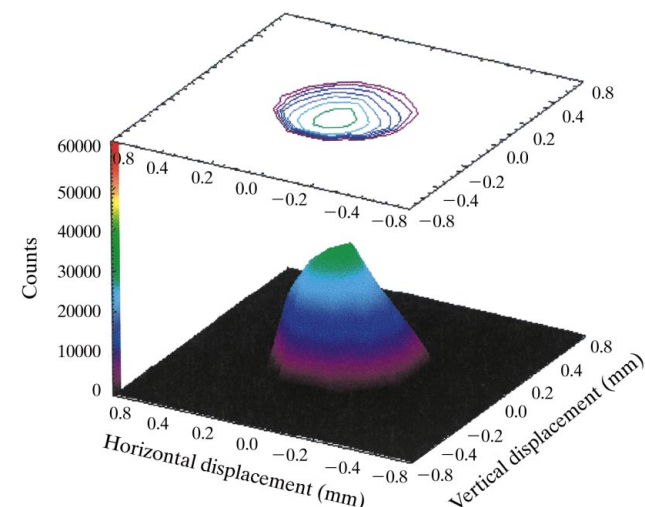


Figure 13
Beam profile of the MSC Blue-2 Optics Configuration.

is unfortunate that one crystal could not be used for the data collection for all the optics configurations tested. However, enough data sets were collected that one can see important trends. The most significant trend is that as intensity increases the data quality improves. However, the MSC Purple-3 Optics Configuration, which produced the highest $\langle I \rangle$ for the proprietary protein, did not produce the best quality data. In order to verify that the crystal had not decayed, we re-collected the data with the MSC Blue-3 Optics Configuration. The results indicate a small degradation in data quality, but the overall $\langle I \rangle$ and $\langle I/\sigma \rangle$ remain constant. Upon inspection of the raw diffraction data, we found that the peaks are at least 2.5 times larger for the MSC Purple-3 Optics Configuration than for the MSC Blue-3 Optics Configuration. The reason for the lower quality for the former is likely to be the result of increased background contribution owing to the larger spot size.

5. Conclusions

It is apparent that the MSC Blue-3 Optics Configuration provides a system with very good qualities. This system provides high useable flux, a clean beam profile, good spectral purity, a small beam size and reasonable divergence for most crystallographic experiments. The MSC Purple-3 Optics Configuration has properties which suggest it is better for small aperture detectors and short crystal-to-detector distances. The MSC/Yale Cross-coupled Optics Configuration gives better divergence characteristics for very long unit cells at the expense of usable flux. It should be noted that the Osmic #1 and #4 optics used were pre-production models and that the Osmic #7 optic was a production model. Current

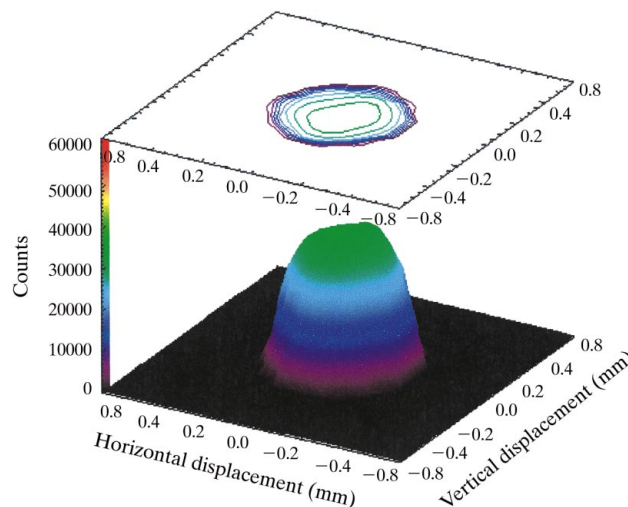


Figure 14
Beam profile of the MSC Blue-3 Optics Configuration.

production model Osmic #4 optics in the MSC Blue-3 Optics Configuration are showing up to twice the total flux as the preproduction model in our laboratory.

We wish to thank Keith Crane and Charlie Stence for designing and manufacturing the alignment hardware and collimators, Paul Swepston, Jim Pflugrath and Cathy Klein for valuable discussions, and Bev Vincent for proofreading the manuscript. We also wish to thank an anonymous MAR user for the myoglobin crystal and the map calculations. Finally, we thank Osmic Inc. for Fig. 1, and Licai Jiang and Rick Smith of Osmic Inc. for useful discussions.

References

- Arndt, U. W. (1990). *J. Appl. Cryst.* **23**, 161–168.
- Arndt, U. W. & Sweet, R. M. (1977). *The Rotation Method in Crystallography*, pp. 45–63. Amsterdam: North-Holland.
- Franks, A. (1955). *Proc. Phys. Soc. London Ser. B*, **68**, 1054–1064.
- Grupido, N. J. & Remus, R. L. (1998). *Laser Focus World*, **3**, 115–117.
- Jiang, L. (1999). Private communication.
- Kirkpatrick, P. & Baez, A. V. (1948). *J. Opt. Soc. Am.* **38**, 766–774.
- McRee, D. E. (1992). *J. Mol. Graph.* **10**, 44–46.
- Otwinowski, Z. & Minor, W. (1997). *Methods Enzymol.* **276**, 307–326.
- Roberts, B. W. & Parrish, W. (1968). *International Tables for X-ray Crystallography*, pp. 73–88. Birmingham: Kynoch Press.
- Schuster, H. & Göbel, H. (1995). *J. Phys. D Appl. Phys.*, pp. 270–275.
- Witz, J. (1969). *Acta Cryst.* **A25**, 30–42.